ACCURACY AND MECHANICAL PROPERTIES OF OPEN-CELL MICROSTRUCTURES FABRICATED BY SELECTIVE LASER SINTERING

S. Eosoly*, G. Ryder†, T. Tansey†, L. Looney*
* School of Mechanical and Manufacturing Engineering, Dublin City University, Dublin, Ireland
†Department of Mechanical Engineering, Institute of Technology Tallaght, Dublin, Ireland

Abstract

This paper investigates the applicability of selective laser sintering (SLS) for the manufacture of scaffold geometries for bone tissue engineering applications. Porous scaffold geometries with open-cell structure and relative density of 10-60 v% were computationally designed and fabricated by selective laser sintering using polyamide powder. Strut and pore sizes ranging from 0.4 - 1 mm and 1.2 -2 mm are explored. The effect of process parameters on compressive properties and accuracy of scaffolds was examined and outline laser power and scan spacing were identified as significant factors. In general, the designed scaffold geometry was not accurately fabricated on the micron-scale. The smallest successfully fabricated strut and pore size was 0.4 mm and 1.2 mm, respectively. It was found that selective laser sintering has the potential to fabricate hard tissue engineering scaffolds. However the technology is not able to replicate exact geometries on the micron-scale but by accounting for errors resulting from the diameter of the laser and from the manufacturing induced geometrical deformations in different building directions, the exact dimensions of the manufactured scaffolds can be predicted and controlled indirectly, which corresponds favorably with its application in computer aided tissue engineering.

Introduction

Tissue engineering aims to produce patient-specific biological substitutes for damaged or lost tissue. One of the principal methods in tissue engineering is to grow the relevant cells in-vitro or in-vivo into the required 3D shape. But cells can only migrate randomly in 2D layers on a surface, therefore 3D porous matrices (scaffolds) with high surface to volume ratio to which the cells can attach and differentiate have been introduced [1-2]. The scaffold aims to mimic the function of the extra cellular matrix (ECM) of the tissue to provide a temporary template for tissue growth. Cells then adhere to the scaffold, proliferate and secrete their own ECM [1-2]. The scaffold has to have an open pore structure to enable tissue ingrowth, vascularisation, and diffusion, it has to serve as an adhesion substrate for the cells, provide temporary mechanical support, and replicate complex anatomical site geometries [3-5].

Conventional technologies of scaffold fabrication like compression molding and particulate leaching, fiber bonding, gas foaming, phase separation, solvent casting and freeze drying often involve the use of porogens and toxic solvents [6]. Many of these conventional scaffold fabrication techniques can only produce scaffolds with limited thickness and random internal architecture that is not reproducible [7]. SLS and other Solid Freeform Fabrication (SFF) technologies are able to overcome these limitations and enable the design and fabrication of scaffolds with predefined internal and external architectures. SLS is an additive particle bonding technique, where a laser beam is used to selectively bond a thin layer of powder particles together [6]. The interaction of the laser beam with the powder raises the powder bed temperature to the melting point and fuses the particles together. When one layer is sintered, a new layer of powder is deposited on top of the existing layer by a roller. This sintering process is repeated until the 3D part is ready. A key advantage of this technology is that a large variety of materials including

biomaterials can be used given that they are available in the form of powder and are not degraded by the laser beam during sintering.

SLS of tissue engineering scaffolds and other porous structures for biomedical applications has been investigated by several groups worldwide. Two main approaches are used to manufacture porous matrices for tissue engineering applications. One uses the fact that laser sintered parts have unintentional, manufacturing-induced porosity that can be governed to some extent by process parameters, particle size and other characteristics of the powder, but the distribution and architecture of the pores are random. Using this method the fabrication of different biocompatible and bioresorbable polymer and polymer/ceramic composites into scaffolds was carried out.

The second approach that will be followed in the present study fabricates scaffolds with complex predesigned internal architectures [8-12]. Williams et al. [8] manufactured scaffolds from Poly(ε-caprolactone) powder with 100μm particle size. Porosity of the designed scaffolds were not accurately reproduced, designed solid regions were incompletely dense with an average porosity of 20%, additionally excess powder was sintered and bonded to the surface of the pore architecture resulting in inaccuracies. The smallest successfully fabricated pore size was 1.75mm in diameter. Partee et al. [9] investigated five process parameters, namely laser power, scan speed, scan spacing, part bed temperature and powder layer delay time at two levels to optimize the parameter settings for the above experiment by applying a 2 level factorial design of experiments. With the found optimal settings the authors could achieve 94% density at the designed solid regions and 3-8% of dimensional accuracy; they were also able to remove most of the excess powder. Das et al. [10] selective laser sintered periodic and biomimetic scaffolds using Nylon 6. Periodic cell based designs with 800μm orthogonal channels, 1200μm pillars, and void fraction of 53.7 % were successfully fabricated using powder with 10-100μm particle size. The biomimetic micro-architectures with 10-100μm features relying on data from μ-CT or μ-MRI of human trabecular bone had to be scaled up (4×) to be able to fabricate them from powder with 38-42μm particle size. Tan et al. [11] fabricated 3D PEEK (25μm) / HA (60μm) composite scaffolds with strut length of 1.5 mm, pore size of 600μm, and porosity less than 80% with microporosity still present within the struts. It was found that microporosity of the struts decreased with increasing HA content.

In the present study the second approach was adopted, that is, the internal architecture of the scaffold geometry is pre-designed. This paper maps the mechanical properties of scaffolds with different relative densities. The effect of different process parameters on accuracy and compressive properties are examined in order to identify the smallest attainable feature size. Both mechanical properties and accuracy are to be examined, since both are of significant importance to the fabrication of successful tissue engineering scaffolds. A small change in the geometry of the scaffold can influence cell interaction during cell culturing, furthermore mechanical properties are also dependent on the geometry of the cellular solid, since even at a given relative density level geometries with different features result in different compressive properties [12]. Therefore accurate geometries with precisely controlled feature shape and size should be manufactured.

Materials and Methods

Polyamide powder marketed under the brand name DuraForm PA was used for this study. DuraForm PA is a white, odorless thermoplastic powder with average particle size of 58μm and rated particle size distribution in which 90% of all particles are between 25-92μm, these values were verified for post-processed powder using a Malvern Mastersizer particle size analyzer.

DuraForm PA is a semi-crystalline polymer with a melting temperature of 184°C. It can be sterilized in an autoclave and is compliant with USP class VI testing.

Sinterstation 2500^{plus} with a low power, λ=10.6 μm continuous wave, CO_2 laser focused to a 400 μm spot was used to fabricate the scaffolds. Prior to the design of experiments, calibration of the SLS system was performed using a millimeter – scaled calibration part and default parameter settings (Table 1a) to identify the necessary shrinkage compensations. The calibration indicated that a shrinkage compensation of 2.9 % is necessary in the X and Y direction, and 2.8 % in the Z direction. After SLS processing was completed, the scaffolds were allowed to cool overnight in the build chamber and were removed from the part bed. Excess powder was brushed off from the exterior and the internal architecture was cleaned using compressed air with a pressure of 2-6 Bars.

Table 1 (a) Default parameter settings for calibration parts, (b) Factors and factor levels used in the Taguchi array

Parameter	Level
Laser fill power	5W
Scan count (fill)	1
Outline laser power	11W
Scan count (outline)	1
Scan spacing	0.15mm
Layer thickness	0.1 mm
Preheat temperature	143 C

Parameter	Lower level	Higher Level
Laser Fill Power	6 W	16 W
Outline laser power	0 W	10 W
Scan spacing	0.1 mm	0.2 mm
Strut size	0.6 mm	0.8mm

The present study carries out 3 sets of experiments. It investigates the effects of relative density (1) and process parameters (2) on the mechanical properties of the scaffolds, and the effect of process parameters on the accuracy (3) of the manufactured parts.

Dependence of mechanical properties on relative density

Applications of scaffolds as temporary bone substitutes in the field of tissue engineering cause them to be loaded in compression, therefore only compressive mechanical properties are studied and evaluated. Disk-shaped scaffold structures (Fig. 1a) with orthogonal channels, designed in SolidWorks 2005 and imported to STL file format were used to investigate the compressive mechanical properties of cellular solids with different relative densities. The strut and pore sizes were alternated between 0.45 – 1 and 1.4 – 1.95 mm respectively to achieve different relative density levels, the range of 40 – 10 v% was examined in 5 v% increments. In order to treat the scaffold structure as a continuum, it had to be ensured that the ratio of specimen diameter to unit cell size was less than 20 [13-14]. At each relative density level five replicates were manufactured at default parameter settings.

Specimens were compressed to failure using an Instron 4202 universal electromechanical testing machine at a rate of 1 mm/s using 50 kN load cell. Compressive Young's modulus and yield strength were determined in accordance with ISO 604:2002 standard. Since in the present experiment series, polyamide was used, which is not a potential material for tissue engineering applications due to lack of bioresorbability, normalized values are being displayed and analyzed. Solid control specimens were manufactured in order to be able to normalize the calculated compressive properties.

Dependence of mechanical properties on process parameters

It is assumed that at a given relative density level the mechanical properties of the specimens can be improved by changing the parameter settings. The examined process parameters were scan spacing, that is the distance between two parallel laser scan lines, laser fill power, that is the

power in watts at which the scan lines are sintered, and outline laser power, that is the power in watts at which the contour of the object is sintered, additionally the strut size of the scaffold was also included in the design.

In order to reduce the number of treatment combinations Taguchi's L8 array was used as a one-half replication of 2^4 full factorial design of experiments to identify the process parameters and interactions that have a significant effect on the mechanical properties. This array enables the examination of 4 factors at two levels including the effects of three interactions. Table 1b summarizes the factors and factor levels that were examined.
Analysis of variance (ANOVA) was accomplished using Design-Expert 7.1 demo version to find the factors significantly affecting the compressive properties of the scaffolds. Disk – shaped lattice geometries (Fig. 1a) with 0.25 relative density were employed to conduct the experiment. Three replicates were fabricated from each treatment combinations, and specimens were compression tested as described above.

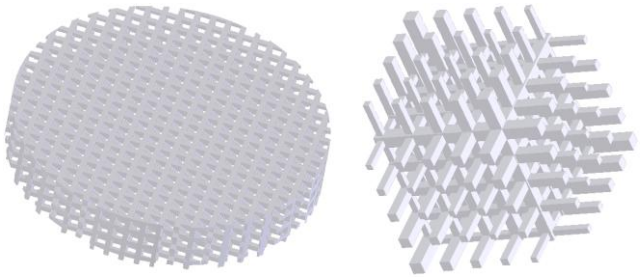

Figure 1 Geometries designed for mechanical testing (a) and accuracy analysis (b)

Dependence of accuracy on process parameters

Accuracy of the manufacturing process was investigated using lattice like scaffolds (Fig. 1b). Geometries (Fig. 1b) were designed with strut sizes of 400µm, 500µm, 600µm, 700µm and 800µm in each of the tree axis planes (XY, XZ, YZ). This resulted in fewer test specimens. The parts were designed in SolidWorks 2005 and exported to the SLS system via the STL format.

The widths of struts were measured from two directions. For example, the widths of the struts built in the Z direction were measured in both the XZ and YZ plane. A micrograph of the strut was taken in both planes using Reichert MeF2 inverted light optical microscope that was then analyzed using Buehler Omnimet Enterprise image analysis software. Grayscale thresholding was executed on the micrographs to separate the struts from the background by representing the two different ranges of grayscale values with different color bitplanes. Binary operations were applied to improve image quality and remove artifacts. Once the borders of the struts were accurately mapped the mean width of the strut was calculated.

Since the goal of the experiment is to identify the process parameters having significant effect on the accuracy of the struts built in X, Y and Z direction, factorial design of experiments was used to examine the effect of 3 process parameters, namely laser fill power, outline laser power and

Table 2 Values of process parameters used in the factorial design of experiment

Factors	Level 1	Level 2	Level 3	Level 4	Level 5
Strut Size	0.4	0.5	0.6	0.7	0.8
Manufacturing direction	X	Y	Z	-	-
Measuring direction	Side1	Side2	-	-	-
Fill Laser Power	6	16	-	-	-
Outline Laser Power	0	10	-	-	-
Scan spacing	0.1	0.2	-	-	-

scan spacing. Table 2 indicates the factors and factor levels of the general factorial design of experiments setup. The design has 240 ($5\times3\times2^4$) different treatment combinations and 3 replicates were manufactured from each treatment combination. The process parameters that are not included in the design were used at their default value. Analysis of variance (ANOVA) was carried out to identify the significant effects of the parameters on the accuracy and compressive properties of the manufactured struts.

Results and Discussions

Dependence of mechanical properties on relative density

Gibson and Ashby discussed [15] that three distinct regions of behavior can be identified as a cellular material is compressed and it was found that the designed scaffolds behave in the exact the same way.

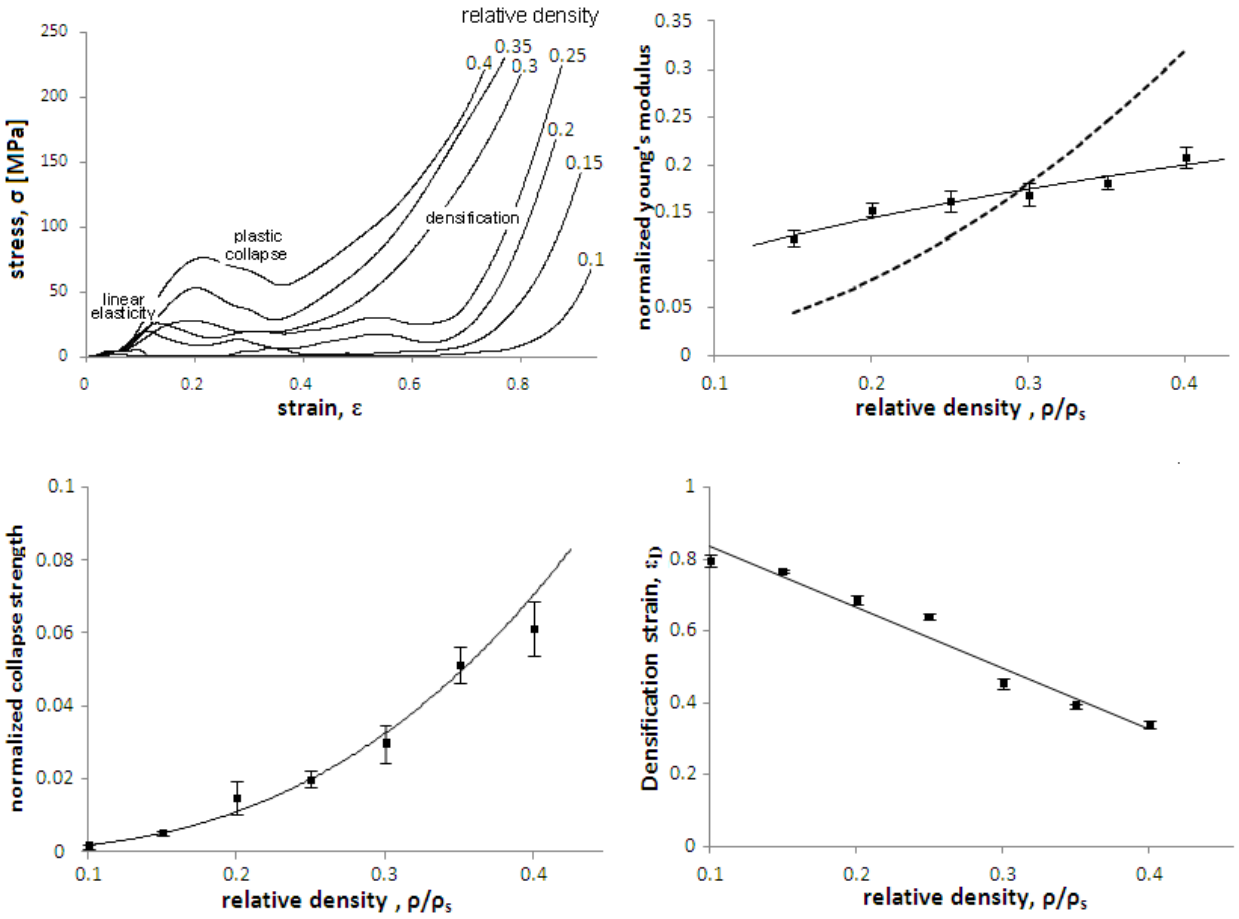

Figure 2 (a) Stress strain map for scaffolds manufactured by SLS, (b) relationship between the relative density and the normalized modulus (continous line – measured data, dotted line – Gibson-Ashby model), (c) relationship between the relative collapse strength and the relative density, (d) relationship between the densifications strain and the relative density of the scaffolds

The stress-strain response of the fabricated scaffolds (Fig. 2a) is shown at different relative density levels, ranging from 0.1-0.4. First a linear elastic slope that is characterized by elastic compression of the struts can be observed at all levels, that is followed by the elastic/plastic collapse region, when the struts buckle and plastic hinges are formed in the structure, further stress compresses the solid material itself, resulting in steep densification. An increase in relative

density of the structure improved the Young's modulus (Fig. 2b), the increase can be described by Eqs. 1.

$$\frac{E}{E_s} = C_1\left(\frac{\rho}{\rho_s}\right)^{k_1} \quad (1)$$

According to Gibson and Ashby's model compressive mechanical properties would improve quadratically (k_1=2) with decreasing porosity. However, measured data deviated from this model. For lower relative densities, when the strut sizes were smaller measured values were significantly higher than predicted by the model, and for high relative densities, when strut sizes were greater measured values were observably lower than predicted resulting in a slower increase (k_1=0.5). This deviation from the model can be attributed to the strut size effect, this will be described in more detail in a later section. As smaller struts appear more dense they therefore have significantly better mechanical properties. C_1 is a constant relating to the geometry and in case of the investigated specimens it was found to be 0.3. This value accounts for both the pre-designed structure and the unintentional manufacturing induced porosity that is present in the designed solid regions.

The increase in relative density elevated the collapse stress as shown in the collapse region of the stress-strain map (Fig. 2a) and in Fig. 2c. The relationship between the collapse stress and the relative density of the structure is given by Eqs. 2.

$$\frac{\sigma_{collapse}}{\sigma_{ys}} = C_2\left(\frac{\rho}{\rho_s}\right)^{k_2} \quad (2)$$

The constants fitting the examined data are k_2=2.5 and C_2=0.8, again the latter constant summarizes the effects of both the designed and manufacturing induced geometry. The relative density increase also resulted in reduced densification strain, as shown in Fig. 2d.

As the relative density increases the densification begins at a lower strain level. The decrease of densification strain as a function of relative density can be described by Eqs. 3 applying the constant C_3=1.7.

$$\varepsilon_D = 1 - C_3\left(\frac{\rho}{\rho_s}\right) \quad (3)$$

As the application of scaffolds is in physiological environment, it must be pointed out that physiological strains are below 1-2%. Therefore from a tissue engineering point of view only the linear elastic region and the collapse stress are relevant, since in case of the examined scaffold structures collapse stress was reached around 2-3% of strain. The above equations govern the behavior of the SLS fabricated scaffold with respect to relative density; however it is hypotized that by altering process parameters at a given relative density level the mechanical properties can be significantly changed.

Dependence of mechanical properties on process parameters

To identify the process parameters that have a significant effect on the compressive properties of the scaffolds laser fill power, outline laser power and scan spacing were simultaneously and systematically varied according to Taguchi's L8 array. Table 3 summarizes the results of the statistical analysis after pooling the most insignificant factors as errors. The F value compares the variance of the model/parameter with the variance of the residuals (difference between experimental data and predicted values). The p value indicates the probability of the model/factor

erroneously being identified as significant. The critical value of p was set to 0.05, no parameter above this value was considered significant.

Table 3 ANOVA tables for the compressive properties (SS - sum of squares, df – degrees of freedom, MS – mean of squares, F – MSmodel/MSresidual, F value, p – probability of seeing the observed F value if there is no factor effect)

ANOVA table for Young's modulus

Source	SS	df	MS	F	p
Model	354.5	4	88.6	16.8	0.021
Outline	100.1	1	100.1	19.0	0.022
FillxOutl	18.4	1	18.4	3.5	0.158
Scan s.	7.2	1	7.2	1.3	0.323
Strut s.	228.7	1	228.7	43.4	0.007
Residual	15.7	3	5.2		
Total	370.37	7			

ANOVA table for yield strength

Source	SS	df	MS	F	p
Model	40.6	3	13.5	21.9	0.006
Outline	25.2	1	25.2	41.0	0.003
Scan s.	7.4	1	7.4	12.1	0.025
Stut s.	7.8	1	7.8	12.7	0.023
Residual	2.4	4	0.6		
Total	43.1	7			

ANOVA confirmed outline laser power and strut size as influential factors for the Young's modulus, and outline laser power, scan spacing and strut size for compressive yield strength. None of the interactions that had been included in the Taguchi array were detected to have any impact on the compressive mechanical properties. The correlation coefficient, which measures the strength of a linear relationship between the experimental data and the predicted values of the regression model for the Young's modulus and the compressive strength, was 0.84 and 0.90 respectively.

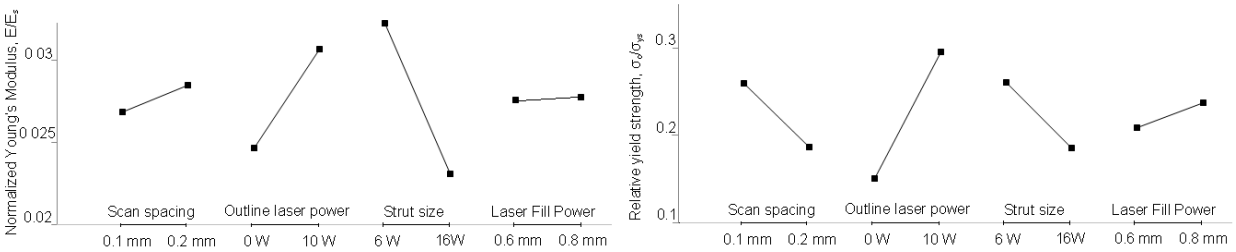

Figure 3 Influence of the design parameters on the mechanical performance (a) Young's modulus and (b) yield strength

Contrary to expectations, at this size level where scan line length is within the range of the laser beam diameter, no effect that can be attributed to the laser fill power was identified. The load bearing struts of the designed disk-shaped scaffolds were fabricated in the Z direction, where the scan line length was 0.6 – 0.8 mm compared to the laser beam diameter of 0.4 mm. It is assumed that the above scan line lengths (0.4 mm) did not trigger the laser.

However outline laser power was detected as a strongly determinative factor, its increased value considerably improved mechanical properties of the tested scaffolds. Increased outline laser power shifts the border of linear elasticity and plastic collapse to the right on the stress-strain map (Fig. 2a) as the linear elastic region becomes steeper and the collapse stress increases resulting in improved modulus and strength values.

Also, measurably improved properties were observed in smaller strut sizes and it is presumed that outline laser power is responsible for the strong strut size effect as scanning electron micrographs revealed that in the struts built in the Z direction only the outline contour was successfully fabricated (Fig. 4). When the same outline laser power was applied on the two different strut sizes (0.6 and 0.8 mm) the effective laser diameter was the same (average 180 μm at 10 W), but

the actual scanned area relative to the whole cross-section of the strut was approximately 20 % higher in the smaller struts (Fig. 4 a, b), this could explain the significant increase in compressive properties for the smaller struts. In struts where the fill laser scan vector length is close to the diameter of the laser beam it would seem that the laser is not triggered. However the outline scan vector is triggered and because the size of the strut is close to the diameter of the laser beam this seems to result in a densely sintered strut, for small strut sizes where the laser beam would overlap as it scans around the outside of the strut. In the case of larger struts, where the fill laser vector has not been triggered, the outline scan vector results in a hollow strut. Furthermore, as previously shown by Cheah et al. [16] when a single line is sintered the start and end portion of the line will be more dense that is caused by the extra deposited surface energy due to the acceleration and deceleration of the laser beam (dwell time). This can also be a possible explanation for the improved mechanical properties of the scaffolds with smaller struts and therefore with shorter scan line lengths.

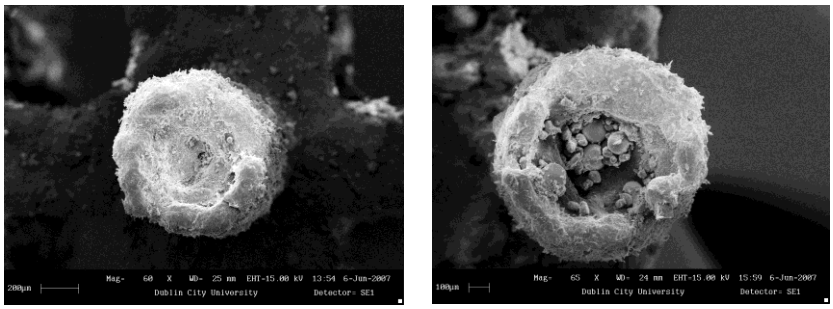

Figure 4 Cross-section of struts fabricated in the Z building direction (a) 0.6 mm, (b) 0.8 mm strut at P_{OI}=10 W

Scan spacing was identified as a process parameter that significantly contributes to the yield strength of the scaffolds indicating the importance of the strength of the structure at the intersection of X, Y and Z struts, where plastic hinges are formed. If scan spacing is reduced the scanned areas will receive significantly higher levels of energy density, which results in the fabrication of denser struts in the X and Y direction, and therefore the collapse stress of the scaffold is elevated. It means that decreasing scan spacing has the same effect on the stress-strain map (Fig. 2a) as increasing the relative density of the scaffold.

There were a number of unexpected results. It was observed that the outline contour in the cross section of the struts built in the Z direction was always present, even in build parameter combinations where the outline laser power was disabled and set to 0 W. However, we were not able to verify that the outline contour is scanned when outline laser power is turned off since if both outline and laser fill power were set to zero, no parts were fabricated.

In the present study only one fabrication direction was examined and only the struts built in the Z direction were loaded. In further studies the effect of different fabrication directions should also be investigated.

Dependence of accuracy on process parameters

Accurate reproduction of the designed scaffolds is essential in order to ensure that the predesigned geometrical features favorable to bone cells during cell culturing and the predicted mechanical properties can be precisely reproduced. Commercial SLS machines are not designed to fabricate geometries with micron-scale features. The smallest attainable feature size is limited by the diameter of the laser that is 0.4 mm but in many cases the scan lines of the 0.4 mm struts did not trigger the laser and these struts were not formed.

In general the geometry of the designed scaffolds was not properly reproduced. All the struts incorporated to the geometry were designed to be prisms with square cross-sections, but none of the fabricated struts reproduced this cross section. Figure 5 shows the typical cross-section of the struts that was attained in the 3 building directions. The designed square cross section has been replicated as a semi-circular (half-moon) cross-section in the X and Y direction and as a circular cross-section in the Z building direction. No significant difference has been detected between the dimensions of the Z struts in the ZY and ZX plane, but the dimensions of the X and Y struts in the XY plane were considerably greater than in the ZX and ZY plane, for the that reason measurements from two sides have been included in the design of experiments.

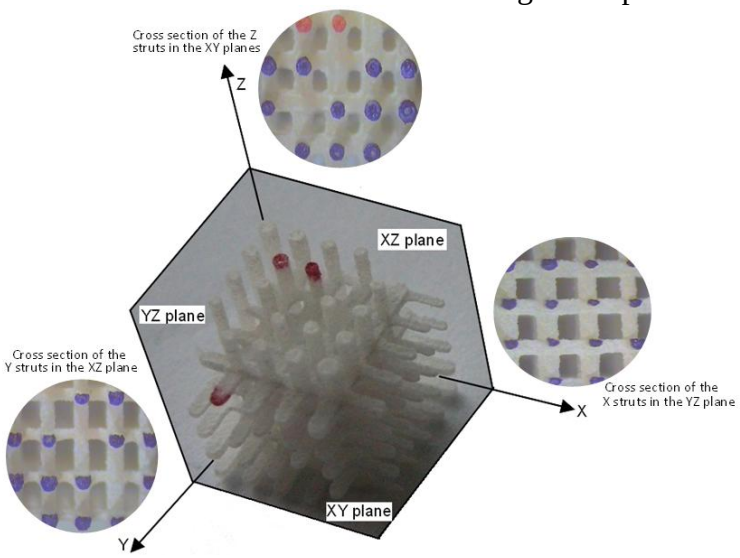

Figure 5 Manufacturing induced deformations in the cross section of the struts in the different building directions

Heat conduction of the powder bed and the laser intensity change along its radius can account for the formation of the semi-circular cross sections in the X and Y direction. Once a layer is sintered, its top surface is plane but the bottom surface curves due to the excess powder sintering around the intentionally sintered layer that distorts the designed geometry in the XZ and YZ plane. Additionally, at the examined size-scale the effect is more pronounced since the laser has a Gaussian intensity distribution along its diameter that results in a strongly curved bottom surface since the scan length is less than two-times the laser diameter. Shrinkage is also present in these struts, less observable than the curvature in the bottom surface but their top surface also becomes concave. The cross sectional difference in the struts manufactured in the Z direction can be explained by the outline scan. In the SEM images (Fig. 4) only the outline scan can be observed, it indicates that the laser might not be triggered when the scan length is between 0.4 and 0.8 mm.

The deviation from the target dimension was between -25% and +35% in the X struts and -5 and +90% in the Y struts, lower values in this range represent the measurement from the XZ and YZ plane respectively, while greater values are from the measurements taken in the XY plane. Deviation of the Z strut dimensions from the designed value was between -10 and 36% in both measuring directions.

Struts of 0.4 mm in size were not fabricated in most cases when the outline laser power was turned off, if fabricated there was observable damage; therefore this strut size was not included in further statistical analysis. By removing the 0.4 mm strut sizes from the model, residuals were significantly reduced and the remaining data better fit the regression curve.

Table 4 presents the ANOVA summary for the accuracy analysis after backward elimination regression with α set to 0.1. Build and measure directions are not real design factors; they were added to the model to be able to include and emphasize the uneven accuracy of the fabricated scaffolds in the different building and measuring directions and to avoid associating the parts with an average value that is less descriptive. Strut size is not a real design factor either, but different levels of this factor were included to verify the significant parameters on the different strut size geometries.

ANOVA detected outline laser power and scan spacing as significant process parameters, one-way interaction between scan spacing and laser fill power were found to be significant, therefore only these parameters and interactions were further analyzed.

Table 4 ANOVA tables for accuracy (SS - sum of squares, df – degrees of freedom, MS – mean of squares, F – MSmodel/MSresidual, F value, p – probability of seeing the observed F value if there is no factor effect)

Source	SS	Df	MS	F	P
Model	3613459	26	138979	43	< 0.0001
A-Strut size	**1520237**	**3**	**506745**	**159**	**< 0.0001**
B-Build direction	647034.9	2	323517	101	< 0.0001
C-Measuring direction	301071	1	301071	94	< 0.0001
D-Laser fill power	6965	1	6965	2	0.1410
E-Outline laser power	**435057**	**1**	**435057**	**136**	**< 0.0001**
F-Scan spacing	**279874**	**1**	**279874**	**87**	**< 0.0001**
AB	93098	6	15516	4	0.0001
AC	29152	3	9717	3	0.0301
BC	58047	2	29023	9	0.0002
BE	57897	2	28948	9	0.0002
BF	23596	2	11798	3	0.0266
CE	34964	1	34964	10	0.0011
DF	**126461**	**1**	**126461**	**39**	**< 0.0001**
Error/Residual	525312	165	3183		
Total	4138772	191			

Influence of scan spacing is more pronounced when the laser fill power is used at its higher level, that is 16W, it explains the significant influence of the one-way interaction between the scan spacing and the laser fill power (DF).

Scan spacing has a constant size decreasing effect on all struts; meaning that as the scan spacing is increased from 0.1 to 0.2 mm, the dimensions of the struts decrease. When accuracy is expressed as percentage deviation from the designed dimension, than scan spacing had a positive effect on the struts manufactured in the Y and Z direction; however it had adverse effect on the X struts, negative in the XZ and positive in the XY plane. The higher energy density supplied to the area in case of lower scan spacing could be an explanation for these accuracy results. However this explanation suggests that laser fill power should also have the same effect on accuracy, but this factor was found to be insignificant at p=0.14 (Table 4).

The importance of outline laser power with respect to the accuracy of the specimens was expected in all directions since the outline contour has an important role in determining the dimensions of the struts. Outline laser power had a constant size increasing effect that in terms of

dimensional deviation was negative on the struts manufactured in the X and Z directions and again adverse on the X struts in the different measuring directions. The width of these struts significantly exceeds the designed width in the XY plane and is measurably below this value in the XZ plane, which is the consequence of the manufacturing induced deformation in the cross - section (square reproduced as half moon) of these struts.

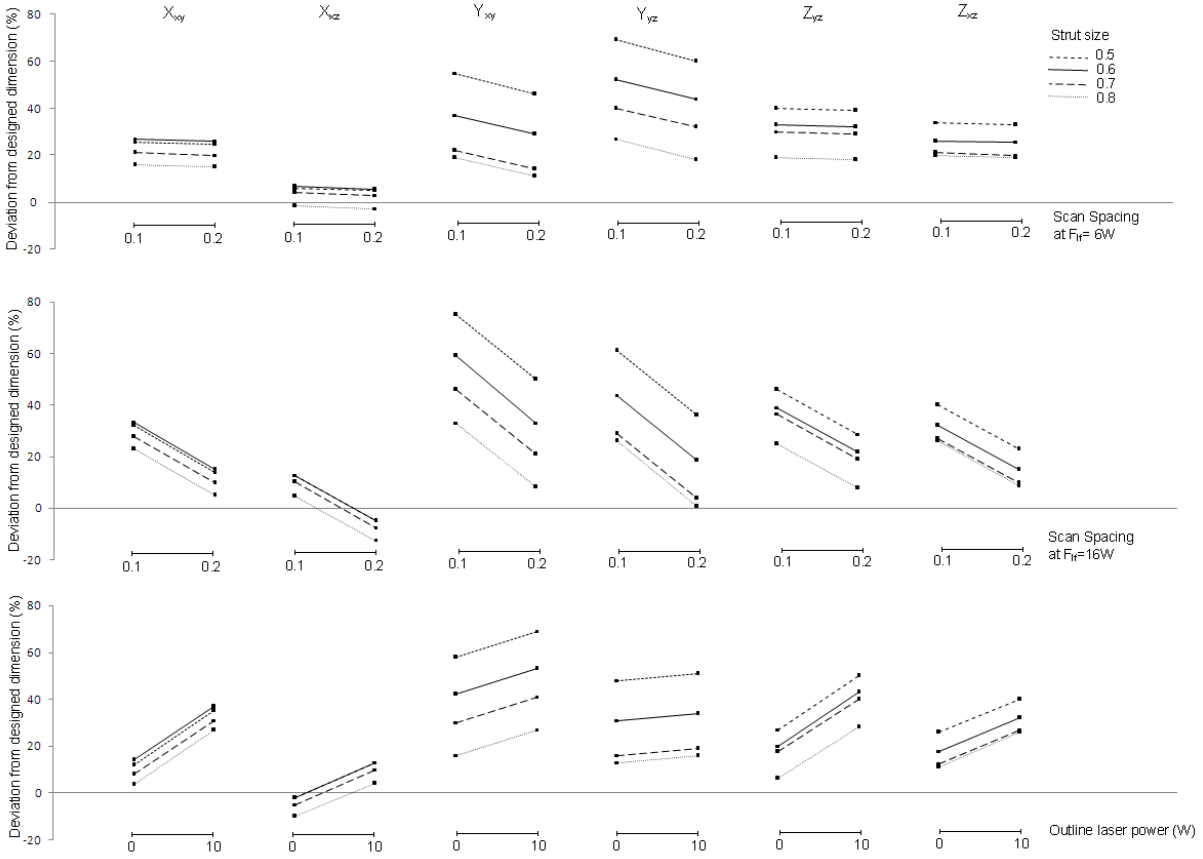

Figure 6 Process parameter effects on different strut sizes in different building and measuring directions, strut size range displayed is from 0.5 – 0.8 mm, target is being 0% of deviation

Conclusions and Further directions

This study investigated the SLS process as a potential manufacturing technology for fabricating hard tissue scaffolds. Mechanical behavior of scaffolds with open-cell internal architecture as a function of relative density was investigated. As a result of the strut size-effect, specific for the manufacturing technology, deviations from prior described model for cellular structures were observed. The dependence of the mechanical properties on the porosity and on processing parameters, namely laser fill power, scan spacing and outline laser power was examined. Scan spacing and outline laser power were detected as significant factors in determining the compressive properties of the manufactured parts. Accuracy of the manufactured struts of 0.4 – 0.8 mm was examined in the different building directions. The cross-sections of the fabricated struts was not properly reproduced, instead of the designed square cross-section they had a semi-circular cross section in the X and Y building directions and a circular cross-section in the Z direction. Other geometries should be examined in order to identify the features that suit the SLS technology the best. It was found that outline laser power and scan spacing are the factors responsible for the accuracy of the scaffolds. The effect of process parameters on the compressive

properties and on the accuracy were only examined at two levels. In further experiments these parameters should be examined at more levels to enable evaluation of not only linear but higher order effects and proper optimization of the process. The effective diameter of the laser should be examined at different laser fill/outline power levels, since the effective laser diameter in part seems to be determining the actual size, density and therefore the mechanical properties of the fabricated scaffolds.

Acknowledgements

This research has been supported by a Marie Curie Early Stage Research Training Fellowship of the European Community's Sixth Framework Programme under contract number MEST-CT-2005-020621.

References

1. BL Seal, TC Otero, A Panitch, Polymeric biomaterials for tissue and organ regeneration, Materials Science and Engineering: R: Reports,31,2001,pp147-230
2. MH Sheridan, LD Shea, MC Peters, DJ Mooney, Bioabsorbable polymer scaffolds for tissue engineering capable of sustained growth factor delivery, J Controlled Release,64,2000, pp91-102
3. KF Leong, CM Cheah, CK Chua, Solid freeform fabrication of three-dimensional scaffolds for engineering replacement tissues and organs, Biomaterials,24,2003,pp2363-78
4. SJ Hollister, RD Maddox, JM Taboas, Optimal design and fabrication of scaffolds to mimic tissue properties and satisfy biological constraints, Biomaterials,23, 2002, pp4095-103
5. RFS Lenza, WL Vasconcelos, JR Jones, LL Hench, Surface-modified 3D scaffolds for tissue engineering, J Mater Sci - Mater Med,13,2002,pp837-42
6. W Yeong, C Chua, K Leong, M Chandrasekaran, Rapid prototyping in tissue engineering: challenges and potential, Trends in Biotechnol,22,2004,pp643-652.
7. S Eosoly, Mechanical testing and finite element modeling of bioresorbable, cellular polymers, Master's Thesis, Budapest, Budapest University of Technology and Economics,2006
8. JM Williams, A Adewunmi, RM Schek, CL Flanagan, PH Krebsbach, SE Feinberg, SJ Hollister, S Das, Bone tissue engineering using polycaprolactone scaffolds fabricated via selective laser sintering, Biomaterials,26,2005,pp4817-27
9. B Partee, SJ Hollister, S Das, Selective Laser Sintering Process Optimization for Layered Manufacturing of CAPA® 6501 Polycaprolactone Bone Tissue Engineering Scaffolds, J Manuf Sci Eng,128,2006,pp.531-40.
10. S Das, JS Hollister, CL Flanagan, A Adewunmi, CK Bark, C Chen, K Ramaswamy, D Rose, E Widjaja, Freeform fabrication of nylon-6 tissue engineering scaffolds, Rapid Prototyping J,9,2003,pp43-49
11. KH Tan, CK Chua, KF Leong, MW Naing, CM Cheah, Fabrication and characterization of three-dimensional poly(ether–ether–ketone)/hydroxyapatite biocomposite scaffolds using laser sintering, Proc Instn Mech Engrs Part H: J Engineering in Medicine,129,2005, pp183-94
12. MH Luxner, J Stampfl, HE Pettermann, linear and non-linear investigation of regular open cell structures, Proceedings of IMECE'04
13. RS Lakes, Size effects and micromechanics of a porous solid. J. Mat. Sci.,18,2572-80,1983
14. R Brezny and DJ Green: The effect of cell size on the mechanical behavior of cellular materials. Acta. Metall. Meter.,38,2517-26,1990
15. LJ Gibson, MF Ashby, Cellular Solids: Structure and Properties, Second Edition Cambridge University Press, Cambridge,1997
16. CM Cheah, KF Leong, CK Chua, KH Low and HS Quek, Characterization of microfeatures in selective laser sintered drug delivery devices, Proc Instn Mech Engrs Part H: J Engineering in Medicine, 216,2002, pp369-83